OPEN ACCESS

University of
BRISTOL

Peer reviewed version

Link to published version (if available):
10.1021/acs.macromol.8b02227

Link to publication record in Explore Bristol Research
PDF-document

University of Bristol - Explore Bristol Research
General rights

Uniform Toroidal Micelles via the Solution Self-Assembly of Block Copolymer – Homopolymer Blends Using a "Frustrated Crystallization" Approach

Huibin Qiu,[†,§,#,*] Alex M. Oliver,[‡,l,#] Jessica Gwyther,[‡,#] Jiandong Cai,[§] Robert L. Harniman,[‡] Dominic W. Hayward,[‡] and Ian Manners[‡,l,*]

[†]School of Chemistry and Chemical Engineering, Shanghai Jiao Tong University, Shanghai 201210, China

[§]School of Physical Science and Technology, ShanghaiTech University, Shanghai 201210, China

[‡]School of Chemistry, University of Bristol, Bristol BS8 1TS, United Kingdom

[l]Department of Chemistry, University of Victoria, Victoria, V8P5C2, Canada

[#] Denotes equal author contributions

[*] To whom correspondence should be addressed, e-mail: hbqiu@sjtu.edu.cn, ian.manners@bristol.ac.uk or imanners@uvic.ca

ABSTRACT

Toroidal nanostructures are of growing importance due to their unique geometry and potential utility in materials fabrication. Although a variety of amphiphilic block copolymers have been shown to self-assemble into toroidal micelles, the conventional methods used are often very slow with little control over the size of the resulting nanostructures. Here, we report a rapid and efficient synthetic route to prepare toroidal micelles of near uniform diameter through the cooperative co-assembly of amorphous blends of polyferrocenylsilane block copolymer and homopolymer, where the degree of polymerization of the core-forming metalloblock in the former is greater than for the latter. The self-assembly process is accomplished within a few minutes and the ring size of the toroids can be varied between 30 and 90 nm by adjusting the mass ratio of the block copolymer and homopolymer. The kinetic stability of the resulting toroidal micelles can be enhanced by frustrating core crystallization through solvent modulation and the toroids can also be readily used as templates to fabricate circular arrays of metal nanoparticles.

INTRODUCTION

Amphiphilic block copolymers (BCPs) self-assemble into a variety of micellar morphologies in selective solvents and the resulting nanoparticles have been shown to be useful in many applications. [1-4] As a result of the kinetically trapped nature of the resulting micelles, the solution processing of BCPs is being increasingly exploited, enabling access to a wide variety of new morphologies. [5] Amongst these, toroidal micelles (ring-like structures) are relatively rare; however, they are of particular interest as their unique geometry is important in a number of biological processes and nanotechnologies. [6-24] For example, DNA molecules collapse from solution to form toroidal condensates and toroids represent a target structure in artificial gene delivery for gene therapy. [6] Various BCP structures have been shown to self-assemble into toroidal micelles, including A–B, [13-16] B–A–B [10-12] and A–B–C, [7-9,15,19,20,22] and graft BCPs. [18,21] In general, careful kinetic control of the assembly process is also required. [6-23] In a few cases, additives such as homopolymers have been found to be useful to promote morphological transformations from rod-like micelles to toroidal micelles. [18, 23] Lin and coworkers used poly(acrylic acid)-*g*-poly(*γ*-benzyl-L-glutamate) PAA-*g*-PBLG graft copolymer and PBLG blends to prepare near monodisperse rods, curved rods and toroids by the dialysis of a solution of molecularly dissolved blend against water over 3 days. [18] Nevertheless, to date, the rapid and convenient formation of morphologically pure toroids of uniform and tunable ring size has been a challenge.

Most examples of BCP toroidal micelles presented in the literature are believed to form via the end-to-end coalescence of cylindrical micelles. In these examples, toroids typically coexist with cylindrical precursors. A lesser-reported alternative pathway has been proposed by He and Schmid [25] using computer simulation whereby a sphere-disc-toroid transition can occur at concentrations close to the critical micelle concentration (CMC). By this route, a spherical micelle first grows into a disc-like micelle followed by nucleation of a hole in the center. Eventually the perforated disc evolves into a toroidal micelle. This growth mechanism is thought to be promoted by a core-forming block with a low glass transition temperature (T_g) and is believed to be operational for PIP-*b*-P2VP (PIP = polyisoprene, P2VP = poly(2-vinylpyridine)) toroid-forming BCPs. [16]

Polyferrocenylsilanes (PFSs) represent a class of main chain metal-containing organosilicon polymers[26] with redox-activity[27,28] and utility for the fabrication of magnetic ceramics[29,30] and catalysts.[31] Generally, PFSs that are unsymmetrically substituted at the Si centers, such as poly(ferrocenylethylmethylsilane) (PFEMS), are amorphous, whereas their symmetrically substituted analogues, for example poly(ferrocenyldimethylsilane) (PFDMS), have been found to crystallize.[26,32-35] BCPs with a crystallizable core-forming PFDMS block are able to form non-spherical micelles such as cylinders and platelets through a process termed crystallization-driven self-assembly (CDSA).[32-35] Over the past decade, we and our collaborators have used CDSA and the "living" characteristics of this process to control micelle dimensions[36-38] and to construct complex PFDMS BCP micellar architectures.[39,40] However, as a result of the presence of crystalline cores, CDSA gives rise to micelles that with high-aspect-ratios that exhibit high stiffness. Consequently, CDSA does not normally favor the formation of vesicles or toroids that possess curved shapes, although limited examples of hollow nanostructures have been reported.[41-43]

When PFDMS BCPs self-assemble in a selective solvent that is very poor for the core-forming metalloblock, spherical micelles with an amorphous core are formed. These often subsequently reassemble into cylindrical or platelets micelles as a consequence of core crystallization.[44-46] An induction period therefore exists prior to the onset of crystallization that provides a window of opportunity in which to self-assemble PFDMS BCPs to form micelles with an amorphous core. On the other hand, the addition of PFDMS homopolymer should, in principle, increase the effective core volume and trigger the formation of micellar structures with low interfacial curvature rather than leading to non-spherical micelles.[13,47] Herein, we report the cooperative co-assembly of blends[13,18,48,49] derived from PFDMS BCP and homopolymer into relatively uniform, size-tunable toroidal micelles. Compared to previously reported routes,[7-23] the present approach is highly convenient and simply involves the injection of a blend of unimers in solution into selective solvents. The resulting toroidal micelles can be subsequently used as templates for the fabrication of nanoparticle arrays. Remarkably, the conditions we use are identical to those previously used to prepare uniform 2D platelets with crystalline cores except that in the latter case, a seeded growth approach was used.[50]

RESULTS

1. Self-Assembly of Potentially Crystallizable Blends of PFDMS$_{36}$-b-P2VP$_{502}$ and PFDMS$_{20}$
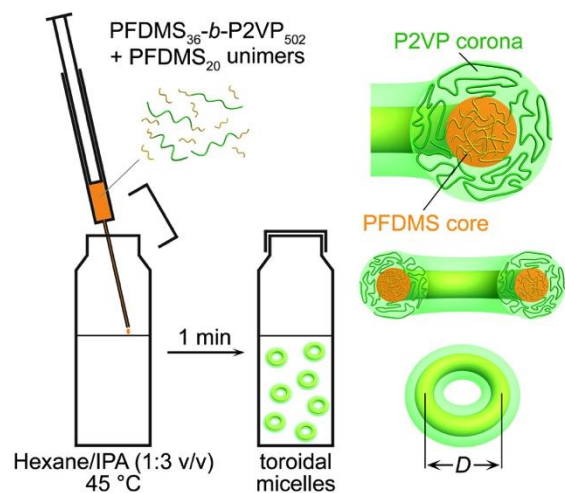
Figure 1. Representative procedure for the formation of toroidal micelles from the blends of PFDMS$_{36}$-b-P2VP$_{502}$ and PFDMS$_{20}$.

For this work we selected a PFDMS-b-P2VP BCP, as this material has previously been shown to undergo a morphological transition from amorphous-core spheres to crystalline-core cylinders depending on the selective solvent used.[45,46] In a typical experiment (Fig. 1), concentrated solutions of PFDMS$_{36}$-b-P2VP$_{502}$ and PFDMS$_{20}$ unimers (in THF, 10 mg/ml) were firstly mixed to give a blend at a specific mass ratio (1:4 – 10:1). An aliquot (5 µL) of the unimeric blend solution was then rapidly injected into a selective solvent mixture of hexane and isopropanol (IPA) (1:3, v/v) at 45 ºC within 1 s and vigorously shaken for 5 s. The assembly process was allowed to proceed for 15 min at 45 ºC before aliquots of the solutions (ca. 15 µL) were drop cast onto carbon coated grids for transmission electron microscopy (TEM) analysis and freshly cleaved mica for atomic force microscopy (AFM) imaging (Fig. 2).

While the blends with a PFDMS$_{36}$-b-P2VP$_{502}$: PFDMS$_{20}$ mass ratio < 2:3 predominantly gave rise to solid spherical nanoparticles (Fig. S1), a reduction in the amount of PFDMS$_{20}$ (mass ratios = 1:1 – 10:1) led to the formation of ring-like micellar structures (Figs. 2a-f). The blend with a 1:1 mass ratio (molar ratio ~1:13) formed uniform toroidal micelles (yield > 80%) with the coexistence of solid

spheres (Fig. 2a). The number-average ring diameter (D_n, Fig. 1) estimated by TEM and AFM was ~70 nm and the size distribution (D_w/D_n) where D_w is the weight-averaged ring diameter was 1.02 (averaged over a minimum of 100 toroids). At BCP : homopolymer mass ratios $\geq$ 2:1, morphologically pure toroidal micelles with narrow size distributions (< 1.02) were observed (Figs. 2b-d). In addition, D_n was found to decrease on reduction of the mass fraction of the PFDMS homopolymer (f_{PFDMS}) as indicated by TEM and AFM (Fig. 2), and dynamic light scattering (DLS, Fig. S2) analyses. Thus, for the PFDMS$_{36}$-b-P2VP$_{502}$ and PFDMS$_{20}$ blend with a 2:1 mass ratio, toroids with D_n = 53 nm were formed (Fig. 2b). In contrast, at mass ratios of 4:1 and 10:1, toroids with a D_n = 37 nm and 30 nm were observed, respectively. The height of the toroidal rim for toroids formed by the blends with a 1:1 and 4:1 ratio was found by AFM to be ~7.5 nm for both samples (Figs. 2e-g).

The resulting toroidal micelles possessed an approximately linear dependence of D_n on the mass fraction of PFDMS homopolymer (f_{PFDMS}) with D_n tunable within a range of ca. 30 – 90 nm (Fig. 2h). Increasing the amount of PFDMS homopolymer in the blend also appeared to increase the effective core volume, as evidenced by the swelling of the ring-shaped PFDMS core (Figs. 2b-d). For example, when comparing Fig. 2d (10:1 mass ratio) with Fig. 2a (1:1 mass ratio) the PFDMS core diameter increased from ~9 nm to ~16 nm as determined by TEM (indicating that the toroidal micelles prefer to adopt a larger ring size to favor a lower degree of interfacial curvature).[47]

For these self-assembly experiments the PFDMS block of the PFDMS$_{36}$-b-P2VP$_{502}$ BCP was designed to be slightly longer than the PFDMS$_{20}$ homopolymer, such that the homopolymer component could be effectively encapsulated in the core of the resulting micelles.[50,51] When blends of PFDMS-b-P2VP BCP and PFDMS homopolymer were used where the PFDMS had a comparable or higher degree of polymerization (DP$_n$, > 40), either spherical micelles or coexisting spheres and toroids were formed (Figs. S3, S4).
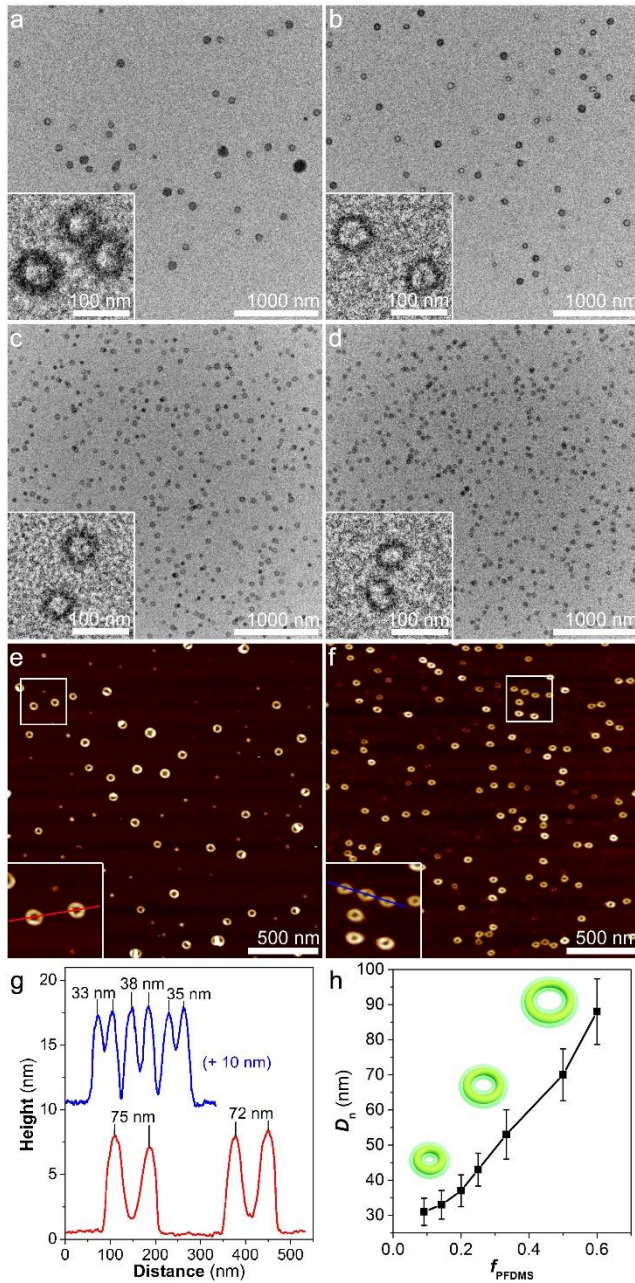
Figure 2. (a-d) TEM images of toroidal micelles after solvent evaporation formed by the co-assembly of PFDMS$_{36}$-*b*-P2VP$_{502}$ and PFDMS$_{20}$ with mass ratio of (a) 1:1, (b) 2:1, (c) 4:1, and (d) 10:1 in 1:3 (v/v) hexane/IPA at 45 °C. (e, f) Corresponding AFM images for the toroidal micelles shown in (a) and (c), respectively. (g) Height profiles for the AFM images shown in (e) (red line, 1:1 ratio) and (f) (blue line, 4:1 ratio). (h) Dependence of D_n on f_{PFDMS} as determined by TEM ($f_{PFDMS} = m_{PFDMS}/(m_{PFDMS} + m_{PFDMS-\textit{b}-P2VP})$, *m* represents the mass of each component). The error bars represent the estimated standard deviations, $\sigma = \sqrt{\sum_{1}^{N}(D_i - D_n)^2/N}$, where *N* is

the total number of toroidal micelles in a survey ($N > 100$), D_i is the diameter of a measured toroidal micelle.

Further experiments showed that the diameter of the toroids also increased with temperature of the selective solvent particularly in the region of 45 – 60 ºC where a difference of ring diameter of ~20 nm was detected by TEM and DLS (Fig. 3, Figs. S5–S7).

The co-assembly of the BCP/homopolymer blends and the micellar morphology adopted was also dependent on the selective solvent composition. In solvents or solvent mixtures that are very poor for PFDMS (see Table S1 for reference), such as methanol, ethanol, IPA, *n*-butanol, and 1:1 (v/v) hexane/acetone, the PFDMS$_{36}$-*b*-P2VP$_{502}$/PFDMS$_{20}$ blends assemble into spherical micelles or aggregate into larger colloidal particles (Fig. S8). In contrast, toroidal micelles emerged in 1:3 (v/v) hexane/methanol and 1:3 (v/v) hexane/ethanol, which are slightly better solvent systems for PFDMS, although the resulting rings were generally small and ill-defined (Fig. S8). Increasing the quality of the solvent mixtures further for the PFDMS block, for example, by the use of 1:3 (v/v) hexane/*n*-butanol, 1:3 (v/v) ethyl acetate/IPA, or 1:4 (v/v) THF/IPA, yielded reasonably well-defined toroidal micelles. However, the ring diameter substantially decreased in 1:1 (v/v) hexane/IPA, indicating a subtle influence modulated by the solvents.
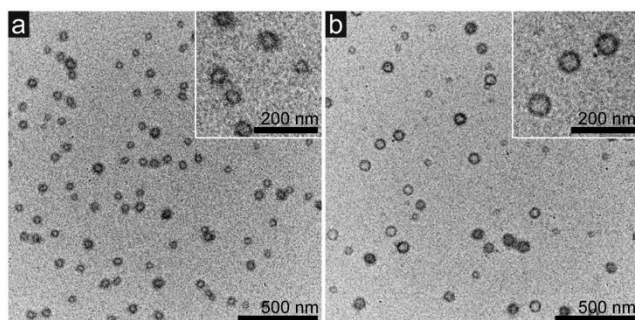

Figure 3. TEM images of toroidal micelles after solvent evaporation formed by the co-assembly of PFDMS$_{36}$-*b*-P2VP$_{502}$ and PFDMS$_{20}$ (mass ratio 4:1) in 1:3 (v/v) hexane/IPA at (a) 23 ºC (D_n = 34 nm) and (b) 60 ºC (D_n = 56 nm).

Compared to other systems,[7-23] the formation of toroidal micelles from the blends of PFDMS$_{36}$-*b*-P2VP$_{502}$ and PFDMS$_{20}$ was surprisingly rapid. Some toroidal micelles could be observed after 1 min

and the self-assembly was generally complete within 5 min (Fig. 4 and Fig. S9). This is substantially different from the conventional toroid micelle systems, where the preparation normally involves low concentrations, elaborate control and lengthy procedures.

The toroidal micelles in Fig. 2 were found to be unstable in hexane/IPA (1:3, v/v), and reassembled into irregular platelets and cylindrical micelles after 1 – 6 h (Fig. 6a, the stability decreased with an increase in f_{PFDMS}). In order to stabilize the toroidal micelles, we explored a "trapping" approach to immobilize the ring structure, either by freezing the core or the corona. The addition of decane (50% v/v) (which is a very poor solvent for the corona-forming P2VP block) following toroid formation led to the aggregation of toroidal micelles into larger solid particles (ca. 120 nm, Fig. S10a). In contrast, in order to trap the PFDMS core, methanol (50% v/v) (a very poor solvent for PFDMS) was added which resulted in an extended lifespan of the toroidal micelles to ~2 days (Fig. S10b). Inspired by these findings, we finally used water, an extremely poor solvent for PFDMS, to frustrate the crystallization of the cores of the toroids. Since hexane is immiscible with water, formation of the toroids was carried out in mixtures of 1:5 v/v THF/IPA. After the addition of water (50% v/v), the toroidal micelles preserved their ring structure and were stable for over 2 months without any aggregation or precipitation.
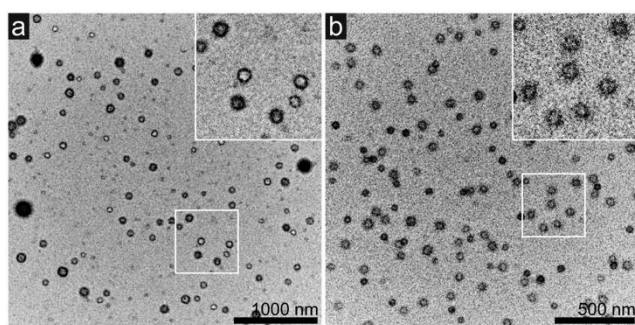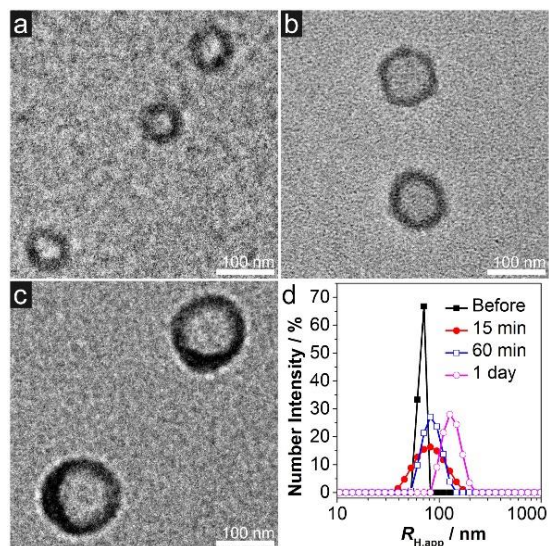

Figure 4. TEM image of toroidal micelles after solvent evaporation formed by the PFDMS$_{36}$-b-P2VP$_{502}$/PFDMS$_{20}$ blends with mass ratio of (a) 2:1 and (b) 4:1 in 1:5 (v/v) THF/IPA at 45 ºC and allowed to age for 5 min.

Interestingly, the diameter of the toroidal micelles, D_n, increased after the addition of water (Fig. 5). As indicated by the TEM images (Fig. 5a-c), the ring diameter increased from ~55 nm to ~115 nm

after 1 day. This was also confirmed by DLS analysis, where the apparent hydrodynamic radius ($R_{H,app}$) almost doubled after 1 day (Fig. 5d). Such an increase of ring size again indicated a complex influence of solvent composition on the structures of the toroidal micelles.

Figure 5. (a) TEM image of toroidal micelles after solvent evaporation formed by the PFDMS$_{36}$-b-P2VP$_{502}$/PFDMS$_{20}$ blends (4:1, mass ratio) in 1:5 (v/v) THF/IPA at 45 ºC and allowed to age for 15 min. (b, c) TEM images of aliquots of the solution after solvent evaporation following the addition of water (50% v/v) and allowed to age for (b) 15 min and (c) 1 day (final volume ratio THF/IPA/water 1:5:6 (v/v)). (d) DLS plots in 1:5 (v/v) THF/IPA of corresponding toroidal micelles before and after the addition of water.

The crystallinity of the PFDMS cores of the toroidal micelles with and without quenching was investigated by solution phase wide-angle X-ray scattering (WAXS) (Fig. 6). The self-assembly of toroidal micelles could be readily scaled and this allowed the successful preparation of concentrated toroid solutions (>8 mg/mL, ca. 1wt% solids, Fig. 6b). Toroidal micelles derived from the co-assembly of the PFDMS$_{36}$-b-P2VP$_{502}$/PFDMS$_{20}$ blends in 1:5 (v/v) THF/IPA that had been allowed to age for 24 h without the addition of water displayed a sharp peak with a d-spacing of 0.65 nm, which is consistent with that for crystalline PFDMS (Figs. 6a,c).[33-35,52] However, the toroidal micelles derived from the co-assembly of the PFDMS$_{36}$-b-P2VP$_{502}$/PFDMS$_{20}$ blends in 1:5 v/v THF/IPA that had been quenched with water (50% v/v) in order to preserve the toroidal structure displayed an

9

amorphous halo with no discernible peaks. The instability of the toroidal micelles is therefore probably a consequence of the crystallization of the PFDMS moieties. Furthermore, these results indicate that the toroidal micelles are intermediate co-assembly products favored by kinetics and that crystallization must be frustrated in order to achieve long-term stability.
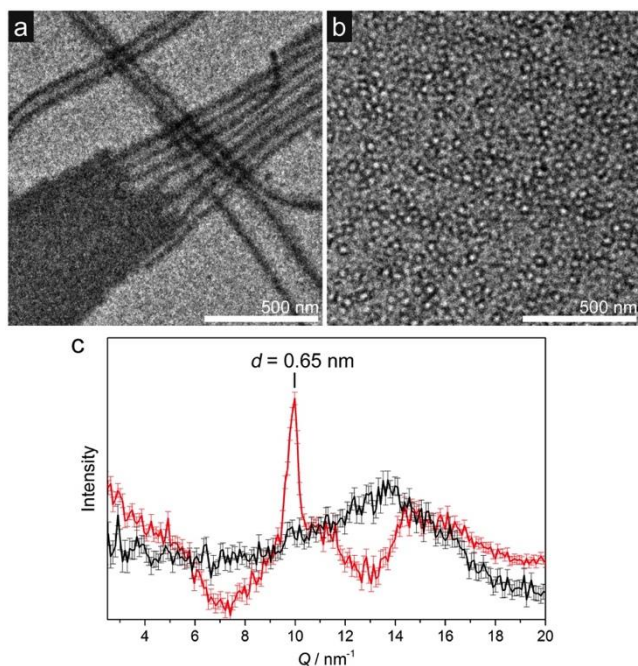
Figure 6. (a) TEM image of an aliquot of the solution after solvent evaporation formed by the injection of 200 µL of solution of mixed PFDMS$_{36}$-*b*-P2VP$_{502}$ and PFDMS$_{20}$ unimers (mass ratios 4:1, overall 50 mg/mL in THF) into 1 mL of 1:5 (v/v) THF/IPA at 45 ºC and allowed to age at 45 ºC for 15 min and at room temperature for 24 h. (b) TEM image of an aliquot of the solution after solvent evaporation formed by the injection of 200 µL of solution of mixed PFDMS$_{36}$-*b*-P2VP$_{502}$ and PFDMS$_{20}$ unimers (mass ratios 4:1, overall 50 mg/mL in THF) into 1 mL of 1:5 (v/v) THF/IPA at 45 ºC and allowing the solution to age at 45 ºC for 15 min followed by the addition of deionized water (50% v/v) and aged at room temperature for 24 h (yielding a concentrated solution of toroidal micelles). (c) WAXS patterns of samples following solvent evaporation shown in (a) (red line) and (b) (black line), respectively.

2. Self-Assembly of Amorphous Blends of PFEMS$_{36}$-*b*-P2VP$_{612}$ and PFEMS$_{23}$

Attempts were made to eliminate the effects of crystallization and hence the need for quenching of the micelles by using amorphous poly(ferrocenylethylmethylsilane) (PFEMS) BCP and atactic homopolymer blends.[26,53] In analogous experiments, unimeric solutions of blends of PFEMS$_{36}$-b-P2VP$_{612}$ and PFEMS$_{23}$ (THF, 10 mg/ml) were mixed at mass ratios of 1:1, 2:1, 4:1 and 10:1. Solutions of the all amorphous blends (5 µL) were injected (1 s) into hexane/IPA (1:3, v/v) selective solvent mixture at 45 °C and shaken for 5 s. The solutions were aged for 15 min at 45 °C before aliquots (ca. 15 µL) were drop cast for TEM analysis. The co-assembly initially formed spherical micelles and relatively irregular ring-like morphologies and it took a much longer period (> 1 day) compared to the PFDMS system to adopt well-defined toroidal structures. Under these conditions, uniform, morphologically pure toroidal micelles were observed for mass ratios = 2:1, 4:1 and 10:1 and remained morphologically stable for at least 6 months in the 1:3 (v/v) hexane/IPA mixture without the need for quenching (Figs. S11, S12).

In a similar way to the crystallizable blend system, the toroidal micelles prepared from the all amorphous PFEMS$_{36}$-b-P2VP$_{612}$ and PFEMS$_{23}$ blends appeared to show a dependence of D_n on the mass fraction of PFEMS homopolymer (f_{PFEMS}) with a narrow size dispersity (< 1.1). At mass ratios of 2:1, 4:1 and 10:1, toroids with a D_n = 72 nm, 57 nm and 48 nm were measured respectively (Figure S11).

3. Functionalization of Toroidal Micelles

The toroidal micelles potentially provide a flexible platform for the fabrication of nanomaterials utilizing both the functional P2VP corona and the redox-reactive PFS core. Gold nanoparticles (NPs) were prepared via the in-situ reduction of NaAuCl$_4$ by NaBH$_4$ in the P2VP corona of the water-trapped toroidal micelles formed by PFDMS$_{36}$-b-P2VP$_{502}$ and PFDMS$_{20}$ blends. Bright- and dark-field TEM images (Fig. 7) revealed the formation of circular arrays of gold NPs (diameter of ca. 4 nm) located in the P2VP corona. This was further confirmed by selected-area energy dispersive X-ray (EDX) spectroscopy analysis (Fig. S13).
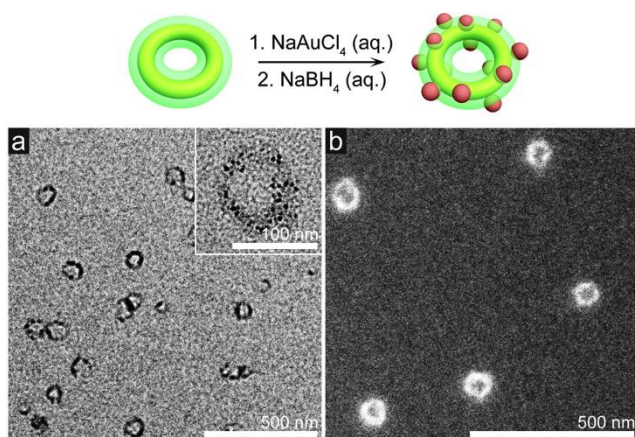
Figure 7. Schematic illustration of the formation of gold NPs by in-situ reduction of NaAuCl₄ in the P2VP corona of water-trapped toroidal micelles derived from the PFDMS₃₆-*b*-P2VP₅₀₂/PFDMS₂₀ blends and corresponding (a) bright filed (inset: higher resolution) and (b) dark field TEM images after solvent evaporation.

DISCUSSION

Our experiments showed the rapid and convenient formation of near-monodisperse toroidal micelles by blending PFDMS₃₆-*b*-P2VP₅₀₂ and PFDMS₂₀ unimers in 1:3 (v/v) hexane/IPA at 45 °C. The formation of this micelle architecture is remarkable as results from previous work using blends both with and without the presence seed micelles are totally different. Previous work using blends of PFDMS-*b*-polyisoprene and PFDMS homopolymer in decane has shown the formation of micelles with elongated planar cores and fiber-like protrusions from the ends.[54] This is an interesting morphological contrast to the amorphous nanostructures that are observed for this work, which may be as a result of the quality of decane for the core-forming block, the altered self-assembly methodology, or the selection of the specific polymers that were used. Furthermore, previous work using the two aforementioned materials studied herein as a unimer blend under seeded growth conditions which were otherwise identical to those used in this study yielded markedly different morphologies. For example, the identical PFDMS₃₆-*b*-P2VP₅₀₂ and PFDMS₂₀ polymers, the same blend ratio, self-assembly solvent system and temperature, with the added incorporation of PFDMS BCP seed micelles to the self-assembly, resulted in the formation of rectangular 2D platelet micelles

with controlled dimensions[50] rather than toroids. The presence of a nucleation point for the unimers to grow off clearly allows the preparation of micelles more typical of those observed with a crystallizable core-forming block. The absence of seeds has a consequence that the PFDMS core-forming block is unable to initially crystallize, resulting in the formation of micelles with an amorphous core.

A number of different factors were shown to alter the size of the toroidal micelles formed. When the amount of PFDMS homopolymer was increased, the number-average ring diameter (D_n) and toroid core width were enlarged (Fig. 2). This is indicative that when there is a greater mass fraction of the PFDMS (f_{PFDMS}), larger ring sizes and micelle core diameters are formed, presumably to accommodate the increase in the core-forming component, which results in a reduction in core-corona interfacial curvature. Furthermore, D_n increased with a rise in temperature used during self-assembly, where a difference of ring diameter of ~20 nm was detected by TEM and DLS (Fig. 3, Figs. S5–S7) in the region of 45 – 60 ºC. We speculate that this may be a consequence of a small degree of confined crystallization of the PFDMS chains on annealing at increased temperatures, which would favor a lower degree of interfacial curvature. The increase in diameter detected in 50% (v/v) water over 1 day (Figure 5) is challenging to explain but may be the result from a similar effect, although an increase in the aggregation number, driven by a desire to decrease the overall surface area of the core exposed to such a poor solvent for PFDMS, cannot be ruled out.

The use of a core-forming block that has the ability to crystallize had a profound effect upon the morphological stability of the micelles. When PFDMS$_{36}$-b-P2VP$_{502}$/PFDMS$_{20}$ blends were used, the toroidal micelles that were initially formed reassembled into irregular platelets and cylindrical micelles after 1 – 6 h (Fig. 6a). The toroids are kinetically trapped nanostructures initially because the solvent system used for the self-assembly is sufficiently poor to inhibit the initial crystallization of the core-forming block. However, slow penetration of the micelle core with solvent would potentially allow the core chains to rearrange and eventually crystallize. This slow crystallization would then dictate the rearrangement of the micelle to form the observed high aspect ratio micelles. This is comparable to previously reported work which observed a slow sphere-to-cylinder transition with

PFDMS-*b*-P2VP BCPs in a solvent that was poor for the core-forming block.[45] The crystallization of the PFDMS core-forming block can effectively be frustrated through the addition of methanol or water. The addition of either of these solvents makes the solvent system poorer for the core which, in turn, further impedes rearrangement and crystallization of the PFDMS chains. When the analogous PFEMS$_{36}$-*b*-P2VP$_{612}$/PFEMS$_{23}$ amorphous blends were used, the micelles were shown to be morphologically stable over several months. The inability of the PFEMS core-forming block to crystallize greatly increases the kinetic stability of the toroids and essentially "freezes" them in that morphology.

Morphologies characterized by the presence of a cavity, such as hollow spheres,[41] nanotubes[41,55,56] and vesicles,[42,57] have been previously prepared with PFDMS BCPs. Moreover, structural reorganization of spherical and cylindrical micelles to form hollow structures has been reported for polylactide BCPs.[43] It is plausible that vesicles rather than toroids might be formed by the blending of BCP and homopolymer experiments described herein. Bright field TEM images show the formation of dark ring structures (Fig. 2a-d), which would signify the formation of a single continuous amorphous PFDMS core associated with toroidal architectures. Toroids prepared with a PFEMS core show the formation of similar ring structures by TEM. (Fig. S11). If vesicles were formed, it would be expected that upon deposition and drying on a TEM grid, nanostructures with roughly even electron contrast across the whole nanostructure would be observed. This would be as a consequence of the collapsed bilayer-type structure in a vesicle, resulting in the PFDMS core essentially covering the entirety of the micelle surface. In addition, AFM height profiles indicate the formation of toroidal structures. The edge of the ring structures (Fig. 2g, ca. 7.5 nm, red trace) is significantly higher than the center (Fig. 2g, ca. 1.5 nm, red trace) due to the presence of the PFDMS core around the circumference of the toroid. The formation of toroidal micelles over vesicles is further substantiated when studying the AFM height profile with the all amorphous PFEMS$_{36}$-*b*-P2VP$_{612}$/PFEMS$_{23}$ (Fig. S12). This shows the height profiles returning to zero at the toroid midpoint, indicative of the formation of ring-like structures. If collapsed vesicles were formed, similar to the evidence provided by TEM, a roughly even height distribution would be expected. The AFM height profiles when PFDMS is used, however,

do not return to the zero value at the toroid midpoint (Fig. 2g, ca. 1.5 nm, red trace). This can be explained as a result of the long $P2VP_{502}$ corona wetting the substrate within the central section of the micelle. This is more apparent when a smaller mass fraction of PFDMS is used as smaller toroids are produced (Fig. 2g, blue trace), which would further crowd the central section of toroids. However, in both cases, there is a clear dip at the midpoint of the micelles, indicative of the formation of a hole within in the micelle structure. Furthermore, other reported examples of BCP toroids that have commensurate diameters to the ones in this report (ca. 70 nm) also showed non-zero heights within the center of the micelles (ca. 2.5 nm at the rim and 0.5 nm at the center).[16]

Previous work on PFDMS-*b*-PDMS BCPs has shown that self-assembled structures can undergo rapid contrast inversion upon irradiation with an electron beam.[58] Therefore, in an attempt to eliminate any effects upon the micelles caused by beam damage and determine whether the structures are as a result of this, a sample of toroids was exposed to a concentrated electron beam for 1 h. However, after both 5 min and 1 h, there was no evidential change in the micelle structures compared to that initially formed (Fig. S14). This indicates that the micelles are not only stable to these conditions, but that the observed structures are not a result of beam damage effects.

There are two previously reported formation mechanisms for the preparation of toroidal micelles.[9,25] The first, by the end-to-end coalescence of cylindrical micelles, is possible for this system. The tendency for PFDMS BCP materials is to form rigid 1D cylinders or 2D platelets when self-assembled as a BCP-homopolymer blend with a crystalline core. If the $PFDMS_{36}$-*b*-$P2VP_{502}$/$PFDMS_{20}$ blends did crystallize, it would not be possible to form toroids by this route as there would be an extreme energy penalty afforded upon bending of the cylinders to yield the high curvature structures. In addition, this effect would also be exacerbated on the length scales of the toroids. However, as the blends studied were shown to be amorphous in the toroids, it is possible that short amorphous cylinders could be formed which could subsequently undergo fusion to form the toroids. However, the alternative mechanism for the preparation of toroids involving the perforation of a spherical/disc-like micelle, is also possible. Nevertheless, due to the rapid nature of the self-assembly, the intermediate nanostructures that would be observed in both these mechanisms could not be detected. It is therefore

possible that the toroids are not formed by either of the two reported mechanisms, and in fact another pathway is operational. Spontaneous cavitation in spherical and cylindrical micelles has been reported upon drying, although, in this case, this was due to hydrogen-bonding interactions between the core and the corona.[43] The rapid process could also be as a result of a unique formation mechanism in contrast with the "ring-closing" or "perforation" models,[9,25] which may be accomplished directly by the co-assembly of blends without any significant morphology transformation. However, to be able to ascertain whether this is the case, the self-assembly of the BCP-homopolymer blends would need to be slowed down significantly and further studies would also be required.

SUMMARY

We have demonstrated a facile and rapid method to prepare uniform toroidal micelles through the co-assembly of a PFS BCP and homopolymer in various solvents, where the degree of polymerization of the core-forming metalloblock in the former is greater than for the latter. The size of the toroids can be effectively tuned through alteration of the BCP-homopolymer blend ratio, or the temperature. The toroidal micelles were either stabilized by a trapping strategy which frustrates the crystallization of the core-forming block, or by using the analogous amorphous PFS polymers. Moreover these nanostructures have been shown as effective platforms for the preparation of hybrid materials, utilizing the corona chemistry to prepare circular arrays of Au NPs.

The mechanism by which the toroids form may involve end-to-end coalescence, the perforation method, or another unknown process and clearly needs further investigation. We anticipate that the cooperative co-assembly method developed in this work should be applicable to other block copolymer and homopolymer blends and thus provides a general strategy to prepare diverse ring-like functional nanostructures. In addition, we are investigating whether toroidal micelles can be used as building blocks for hierarchical self-assembly with other BCP micelles and the longer term dimensional changes that occur as the systems evolve in certain solvents such as water..

ASSOCIATED CONTENT

16

Supporting Information. Experimental details and additional results. This material is available free of charge via the Internet at http://pubs.acs.org.

AUTHOR INFORMATION

Corresponding Author

hbqiu@sjtu.edu.cn; ian.manners@bristol.ac.uk, imanners@uvic.ca

Author Contributions

# These authors contributed equally.

REFERENCES

1.   Mai, Y.; Eisenberg, A., Self-assembly of block copolymers. *Chem. Soc. Rev.* **2012**, *41* (18), 5969-85.
2.   Tritschler, U.; Pearce, S.; Gwyther, J.; Whittell, G. R.; Manners, I., 50th Anniversary Perspective: Functional Nanoparticles from the Solution Self-Assembly of Block Copolymers. *Macromolecules* **2017**, *50* (9), 3439-3463.
3.   Lodge, T. P., Block Copolymers: Past Successes and Future Challenges. *Macromol. Chem. Phys.* **2003**, *204* (2), 265-273.
4.   Dong, C.-M.; Liu, G., Linear–dendritic biodegradable block copolymers: from synthesis to application in bionanotechnology. *Polym. Chem.* **2013**, *4* (1), 46-52.
5.   Hayward, R. C.; Pochan, D. J., Tailored Assemblies of Block Copolymers in Solution: It Is All about the Process. *Macromolecules* **2010**, *43* (8), 3577-3584.
6.   Conwell, C. C.; Vilfan, I. D.; Hud, N. V., Controlling the size of nanoscale toroidal DNA condensates with static curvature and ionic strength. *PNAS* **2003**, *100* (16), 9296-9301.
7.   Pochan, D. J.; Chen, Z.; Cui, H.; Hales, K.; Qi, K.; Wooley, K. L., Toroidal Triblock Copolymer Assemblies. *Science* **2004**, *306* (5693), 94-97.
8.   Chen, Z.; Cui, H.; Hales, K.; Li, Z.; Qi, K.; Pochan, D. J.; Wooley, K. L., Unique Toroidal Morphology from Composition and Sequence Control of Triblock Copolymers. *J. Am. Chem. Soc.* **2005**, *127* (24), 8592-8593.
9.   Cui, H.; Chen, Z.; Wooley, K. L.; Pochan, D. J., Origins of toroidal micelle formation through charged triblock copolymer self-assembly. *Soft Matter* **2009**, *5* (6), 1269-1278.
10.   Zhu, J.; Liao, Y.; Jiang, W., Ring-Shaped Morphology of "Crew-Cut" Aggregates from ABA Amphiphilic Triblock Copolymer in a Dilute Solution. *Langmuir* **2004**, *20* (9), 3809-3812.
11.   Yu, H.; Jiang, W., Effect of Shear Flow on the Formation of Ring-Shaped ABA Amphiphilic Triblock Copolymer Micelles. *Macromolecules* **2009**, *42* (9), 3399-3404.
12.   Wang, Z.; Jiang, W., Temperature-induced reversible transformation between toroidal and cylindrical assemblies under shear flow. *Soft Matter* **2010**, *6* (16), 3743–3746.
13.   Ouarti, N.; Viville, P.; Lazzaroni, R.; Minatti, E.; Schappacher, M.; Deffieux, A.; Borsali, R., Control of the Morphology of Linear and Cyclic PS-*b*-PI Block Copolymer Micelles via PS Addition. *Langmuir* **2005**, *21* (4), 1180-1186.
14.   LaRue, I.; Adam, M.; Pitsikalis, M.; Hadjichristidis, N.; Rubinstein, M.; Sheiko, S. S., Reversible Morphological Transitions of Polystyrene-*b*-polyisoprene Micelles. *Macromolecules* **2006**, *39* (1), 309-314.

15. Liu, Y.-L.; Chang, Y.-H.; Chen, W.-H., Preparation and Self-Assembled Toroids of Amphiphilic Polystyrene-C60-Poly(N-isopropylacrylamide) Block Copolymers. *Macromolecules* **2008,** *41* (21), 7857-7862.

16. Huang, H.; Chung, B.; Jung, J.; Park, H. W.; Chang, T., Toroidal micelles of uniform size from diblock copolymers. *Angew. Chem., Int. Ed.* **2009,** *48* (25), 4594-4597.

17. Liu, C.; Chen, G.; Sun, H.; Xu, J.; Feng, Y.; Zhang, Z.; Wu, T.; Chen, H., Toroidal Micelles of Polystyrene-*block*-Poly(acrylic acid). *Small* **2011,** *7* (19), 2721-2726.

18. Chen, L.; Jiang, T.; Lin, J.; Cai, C., Toroid formation through self-assembly of graft copolymer and homopolymer mixtures: experimental studies and dissipative particle dynamics simulations. *Langmuir* **2013,** *29* (26), 8417-26.

19. Li, X.; Gao, Y.; Xing, X.; Liu, G., Polygonal Micellar Aggregates of a Triblock Terpolymer Containing a Liquid Crystalline Block. *Macromolecules* **2013,** *46* (18), 7436-7442.

20. Xiao, X.; He, S.; Dan, M.; Huo, F.; Zhang, W., Nanoparticle-to-vesicle and nanoparticle-to-toroid transitions of pH-sensitive ABC triblock copolymers by in-to-out switch. *Chem. Commun.* **2014,** *50* (30), 3969-3972.

21. Luo, H.; Santos, J. L.; Herrera-Alonso, M., Toroidal structures from brush amphiphiles. *Chem. Commun.* **2014,** *50* (5), 536-538.

22. Ni, B.; Huang, M.; Chen, Z.; Chen, Y.; Hsu, C. H.; Li, Y.; Pochan, D.; Zhang, W. B.; Cheng, S. Z.; Dong, X. H., Pathway toward large two-dimensional hexagonally patterned colloidal nanosheets in solution. *J. Am. Chem. Soc.* **2015,** *137* (4), 1392-1395.

23. Yang, C.; Gao, L.; Lin, J.; Wang, L.; Cai, C.; Wei, Y.; Li, Z., Toroid Formation through a Supramolecular "Cyclization Reaction" of Rodlike Micelles. *Angew. Chem., Int. Ed.* **2017,** *56* (20), 5546-5550.

24. Cai, J.; Mineart, K. P.; Li, X.; Spontak, R. J.; Manners, I.; Qiu, H., Hierarchical Self-Assembly of Toroidal Micelles into Multidimensional Nanoporous Superstructures. *ACS Macro Letters* **2018,** *7* (8), 1040-1045.

25. He, X.; Schmid, F., Spontaneous formation of complex micelles from a homogeneous solution. *Phys. Rev. Lett.* **2008,** *100* (13), 137802.

26. Hailes, R. L.; Oliver, A. M.; Gwyther, J.; Whittell, G. R.; Manners, I., Polyferrocenylsilanes: synthesis, properties, and applications. *Chem. Soc. Rev.* **2016,** *45* (19), 5358-5407.

27. Ma, Y.; Dong, W. F.; Hempenius, M. A.; Mohwald, H.; Vancso, G. J., Redox-controlled molecular permeability of composite-wall microcapsules. *Nat. Mater.* **2006,** *5* (9), 724-729.

28. Arsenault, A. C.; Puzzo, D. P.; Manners, I.; Ozin, G. A., Photonic-crystal full-colour displays. *Nat. Photon.* **2007,** *1* (8), 468-472.

29. MacLachlan, M. J.; Ginzburg, M.; Coombs, N.; Raju, N. P.; Greedan, J. E.; Ozin, G. A.; Manners, I., Superparamagnetic Ceramic Nanocomposites: Synthesis and Pyrolysis of Ring-Opened Poly(ferrocenylsilanes) inside Periodic Mesoporous Silica. *J. Am. Chem. Soc.* **2000,** *122* (16), 3878-3891.

30. Ginzburg, M.; MacLachlan, M. J.; Yang, S. M.; Coombs, N.; Coyle, T. W.; Raju, N. P.; Greedan, J. E.; Herber, R. H.; Ozin, G. A.; Manners, I., Genesis of Nanostructured, Magnetically Tunable Ceramics from the Pyrolysis of Cross-Linked Polyferrocenylsilane Networks and Formation of Shaped Macroscopic Objects and Micron Scale Patterns by Micromolding Inside Silicon Wafers. *J. Am. Chem. Soc.* **2002,** *124* (11), 2625-2639.

31. Hinderling, C.; Keles, Y.; Stöckli, T.; Knapp, H. F.; de los Arcos, T.; Oelhafen, P.; Korczagin, I.; Hempenius, M. A.; Vancso, G. J.; Pugin, R.; Heinzelmann, H., Organometallic Block Copolymers as Catalyst Precursors for Templated Carbon Nanotube Growth. *Adv. Mater.* **2004,** *16* (11), 876-879.

32. Massey, J. A.; Temple, K.; Cao, L.; Rharbi, Y.; Raez, J.; Winnik, M. A.; Manners, I., Self-Assembly of Organometallic Block Copolymers: The Role of Crystallinity of the Core-Forming Polyferrocene Block in the Micellar Morphologies Formed by Poly(ferrocenylsilane-*b*-dimethylsiloxane) in n-Alkane Solvents. *J. Am. Chem. Soc.* **2000,** *122* (47), 11577-11584.

33. Lammertink, R. G. H.; Hempenius, M. A.; Manners, I.; Vancso, G. J., Crystallization and Melting Behavior of Poly(ferrocenyldimethylsilanes) Obtained by Anionic Polymerization. *Macromolecules* **1998,** *31* (3), 795-800.

34. Papkov, V. S.; Gerasimov, M. V.; Dubovik, I. I.; Sharma, S.; Dementiev, V. V.; Pannell, K. H., Crystalline Structure of Some Poly(ferrocenylenedialkylsilylenes). *Macromolecules* **2000,** *33* (19), 7107-7115.

35. Chen, Z.; Foster, M. D.; Zhou, W.; Fong, H.; Reneker, D. H.; Resendes, R.; Manners, I., Structure of Poly(ferrocenyldimethylsilane) in Electrospun Nanofibers. *Macromolecules* **2001,** *34* (18), 6156-6158.

36. Wang, X.; Guerin, G.; Wang, H.; Wang, Y.; Manners, I.; Winnik, M. A., Cylindrical Block Copolymer Micelles and Co-Micelles of Controlled Length and Architecture. *Science* **2007,** *317* (5838), 644-647.

37. Gilroy, J. B.; Gadt, T.; Whittell, G. R.; Chabanne, L.; Mitchels, J. M.; Richardson, R. M.; Winnik, M. A.; Manners, I., Monodisperse cylindrical micelles by crystallization-driven living self-assembly. *Nat. Chem.* **2010,** *2* (7), 566-570.

38. Hudson, Z. M.; Boott, C. E.; Robinson, M. E.; Rupar, P. A.; Winnik, M. A.; Manners, I., Tailored hierarchical micelle architectures using living crystallization-driven self-assembly in two dimensions. *Nat. Chem.* **2014,** *6*, 893-898.

39. Qiu, H.; Hudson, Z. M.; Winnik, M. A.; Manners, I., Multidimensional hierarchical self-assembly of amphiphilic cylindrical block comicelles. *Science* **2015,** *347* (6228), 1329-1332.

40. Li, X.; Gao, Y.; Boott, C. E.; Winnik, M. A.; Manners, I., Non-covalent synthesis of supermicelles with complex architectures using spatially confined hydrogen-bonding interactions. *Nat. Commun.* **2015,** *6*, 8127.

41. Raez, J.; Manners, I.; Winnik, M. A., Nanotubes from the Self-Assembly of Asymmetric Crystalline−Coil Poly(ferrocenylsilane−siloxane) Block Copolymers. *J. Am. Chem. Soc.* **2002,** *124* (35), 10381-10395.

42. Schacher, F. H.; Elbert, J.; Patra, S. K.; Yusoff, S. F.; Winnik, M. A.; Manners, I., Responsive vesicles from the self-assembly of crystalline-coil polyferrocenylsilane-*block*-poly(ethylene oxide) star-block copolymers. *Chemistry* **2012,** *18* (2), 517-25.

18

43.   Petzetakis, N.; Robin, M. P.; Patterson, J. P.; Kelley, E. G.; Cotanda, P.; Bomans, P. H. H.; Sommerdijk, N. A. J. M.; Dove, A. P.; Epps, T. H.; O'Reilly, R. K., Hollow Block Copolymer Nanoparticles through a Spontaneous One-step Structural Reorganization. *ACS Nano* **2013,** *7* (2), 1120-1128.

44.   Wang, H.; Winnik, M. A.; Manners, I., Synthesis and Self-Assembly of Poly(ferrocenyldimethylsilane-*b*-2-vinylpyridine) Diblock Copolymers. *Macromolecules* **2007,** *40* (10), 3784-3789.

45.   Shen, L.; Wang, H.; Guerin, G.; Wu, C.; Manners, I.; Winnik, M. A., A Micellar Sphere-to-Cylinder Transition of Poly(ferrocenyldimethylsilane-*b*-2-vinylpyridine) in a Selective Solvent Driven by Crystallization. *Macromolecules* **2008,** *41* (12), 4380-4389.

46.   Hsiao, M.-S.; Yusoff, S. F. M.; Winnik, M. A.; Manners, I., Crystallization-Driven Self-Assembly of Block Copolymers with a Short Crystallizable Core-Forming Segment: Controlling Micelle Morphology through the Influence of Molar Mass and Solvent Selectivity. *Macromolecules* **2014,** *47* (7), 2361-2372.

47.   Smart, T.; Lomas, H.; Massignani, M.; Flores-Merino, M. V.; Perez, L. R.; Battaglia, G., Block copolymer nanostructures. *Nano Today* **2008,** *3* (3-4), 38-46.

48.   Wright, D. B.; Patterson, J. P.; Pitto-Barry, A.; Lu, A.; Kirby, N.; Gianneschi, N. C.; Chassenieux, C.; Colombani, O.; O'Reilly, R. K., The Copolymer Blending Method: A New Approach for Targeted Assembly of Micellar Nanoparticles. *Macromolecules* **2015,** *48* (18), 6516-6522.

49.   Zhu, J.; Zhang, S.; Zhang, K.; Wang, X.; Mays, J. W.; Wooley, K. L.; Pochan, D. J., Disk-cylinder and disk-sphere nanoparticles via a block copolymer blend solution construction. *Nat. Commun.* **2013,** *4*, 2297.

50.   Qiu, H.; Gao, Y.; Boott, C. E.; Gould, O. E. C.; Harniman, R. L.; Miles, M. J.; Webb, S. E. D.; Winnik, M. A.; Manners, I., Uniform patchy and hollow rectangular platelet micelles from crystallizable polymer blends. *Science* **2016,** *352* (6286), 697-701.

51.   Qiu, H.; Cambridge, G.; Winnik, M. A.; Manners, I., Multi-armed micelles and block co-micelles via crystallization-driven self-assembly with homopolymer nanocrystals as initiators. *J. Am. Chem. Soc.* **2013,** *135* (33), 12180-3.

52.   Gilroy, J. B.; Rupar, P. A.; Whittell, G. R.; Chabanne, L.; Terrill, N. J.; Winnik, M. A.; Manners, I.; Richardson, R. M., Probing the structure of the crystalline core of field-aligned, monodisperse, cylindrical polyisoprene-*block*-polyferrocenylsilane micelles in solution using synchrotron small- and wide-angle X-ray scattering. *J. Am. Chem. Soc.* **2011,** *133* (42), 17056-17062.

53.   Rider, D. A.; Cavicchi, K. A.; Power-Billard, K. N.; Russell, T. P.; Manners, I., Diblock Copolymers with Amorphous Atactic Polyferrocenylsilane Blocks: Synthesis, Characterization, and Self-Assembly of Polystyrene-*block*-poly(ferrocenylethylmethylsilane) in the Bulk State. *Macromolecules* **2005,** *38* (16), 6931-6938.

54.   Cambridge, G.; Gonzalez-Alvarez, M. J.; Guerin, G.; Manners, I.; Winnik, M. A., Solution Self-Assembly of Blends of Crystalline-Coil Polyferrocenylsilane-*block*-polyisoprene with Crystallizable Polyferrocenylsilane Homopolymer. *Macromolecules* **2015,** *48* (3), 707-716.

55.   Wang, X.; Wang, H.; Frankowski, D. J.; Lam, P. G.; Welch, P. M.; Winnik, M. A.; Hartmann, J.; Manners, I.; Spontak, R. J., Growth and Crystallization of Metal-Containing Block Copolymer Nanotubes in a Selective Solvent. *Adv. Mater.* **2007,** *19* (17), 2279-2285.

56.   Frankowski, D. J.; Raez, J.; Manners, I.; Winnik, M. A.; Khan, S. A.; Spontak, R. J., Formation of Dispersed Nanostructures from Poly(ferrocenyldimethylsilane-*b*-dimethylsiloxane) Nanotubes upon Exposure to Supercritical Carbon Dioxide. *Langmuir* **2004,** *20* (21), 9304-9314.

57.   Power-Billard, K. N.; Spontak, R. J.; Manners, I., Redox-Active Organometallic Vesicles: Aqueous Self-Assembly of a Diblock Copolymer with a Hydrophilic Polyferrocenylsilane Polyelectrolyte Block. *Angew. Chem., Int. Ed.* **2004,** *43* (10), 1260-1264.

58.   Wang, Y.; Coombs, N.; Manners, I.; Winnik, M. A., Contrast Inversion in TEM Studies of Poly(ferrocenylsilane)-*block*-Poly(dimethylsiloxane) Diblock Copolymers. *Macromol. Chem. Phys.* **2008,** *209* (14), 1432-1436.